Immunity, Volume *33*

Supplemental Information

Mzb1 Protein Regulates Calcium Homeostasis, Antibody Secretion, and Integrin Activation in Innate-like B Cells

Henrik Flach, Marc Rosenbaum, Marlena Duchniewicz, Sola Kim, Shenyuan L. Zhang, Michael D. Cahalan, Gerhard Mittler, and Rudolf Grosschedl

Inventory:

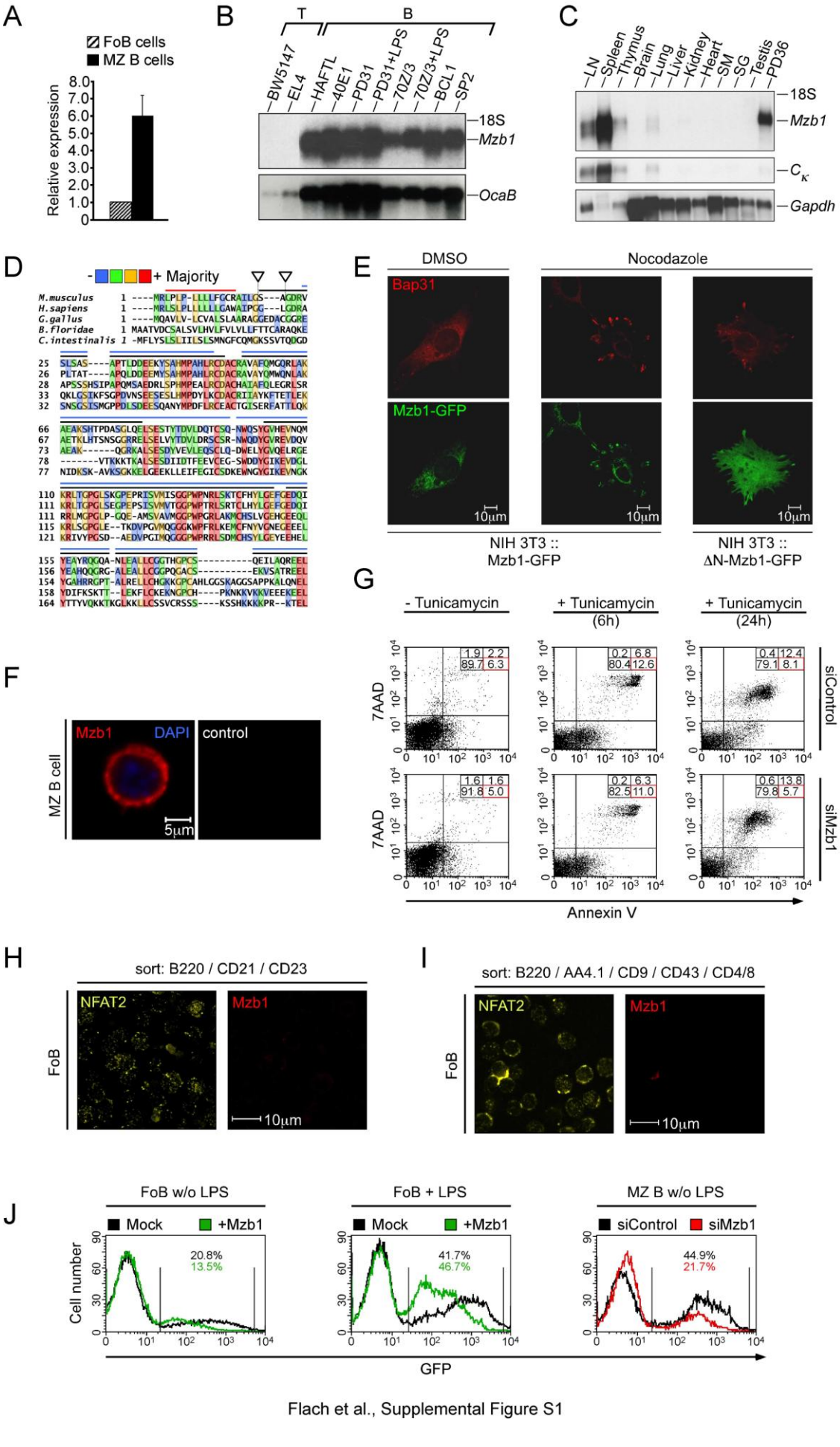

Flach et al., Supplemental Figure S1

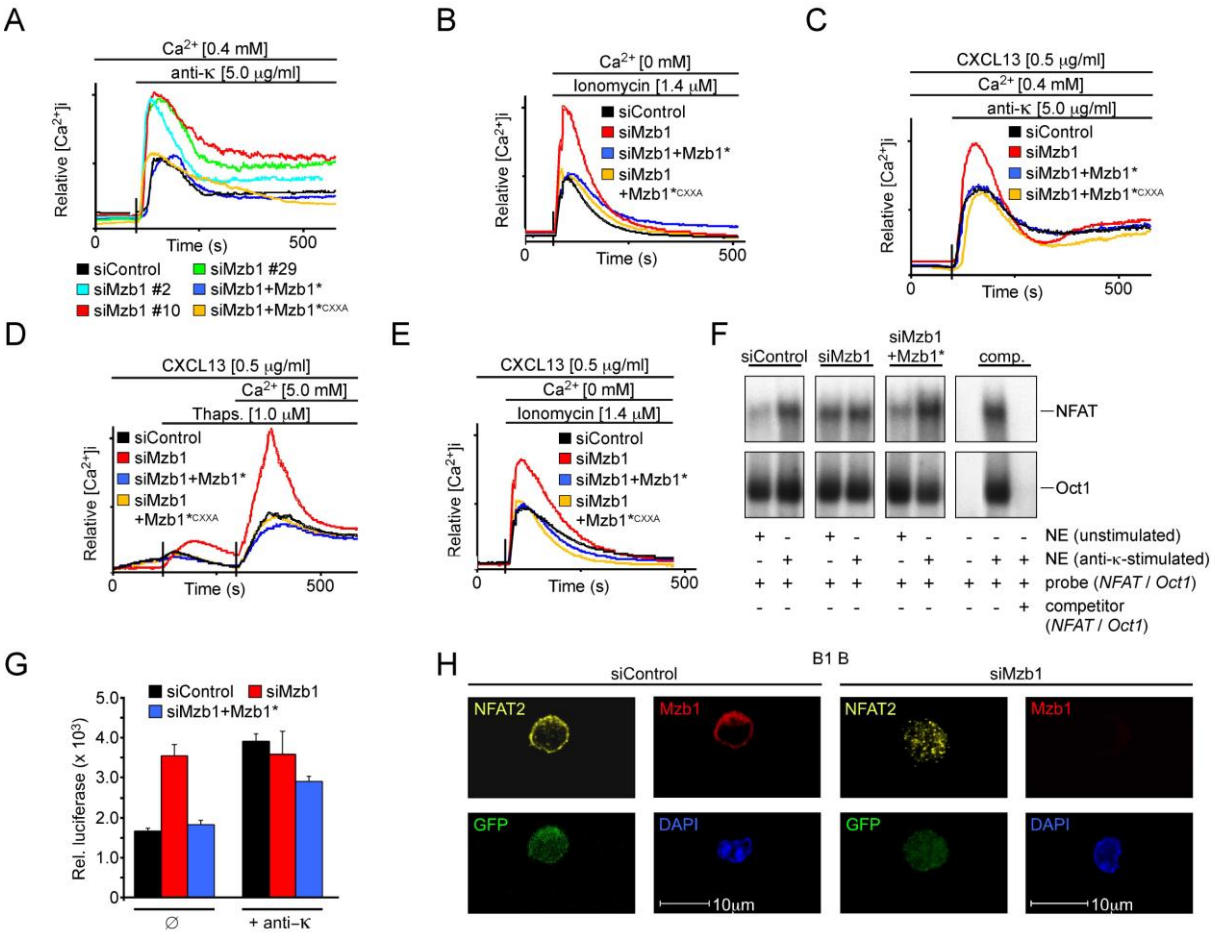

Flach et al., Supplemental Figure S2

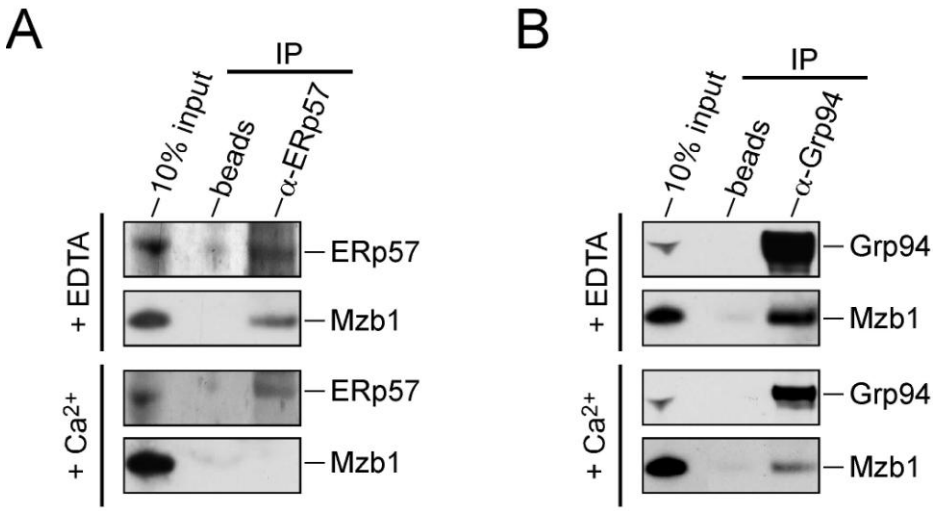

Flach et al., Supplemental Figure S3

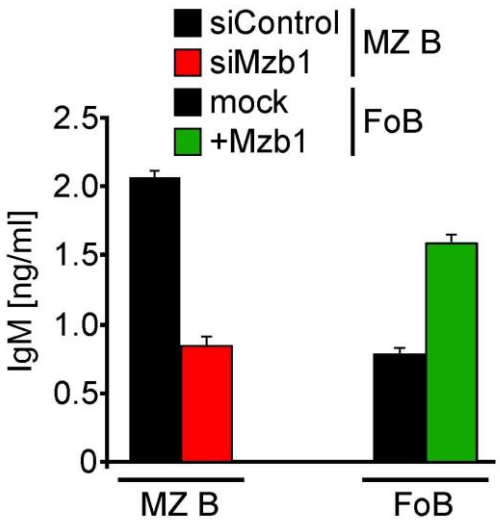

Flach et al., Supplemental Figure S4

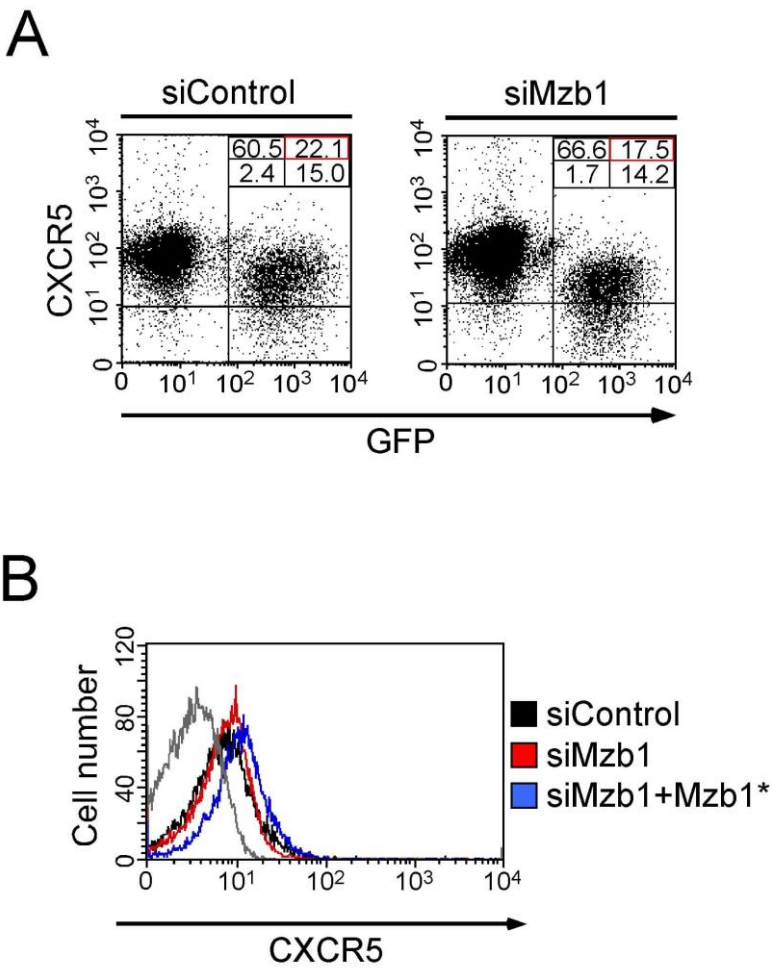

Flach et al., Supplemental Fig. S5

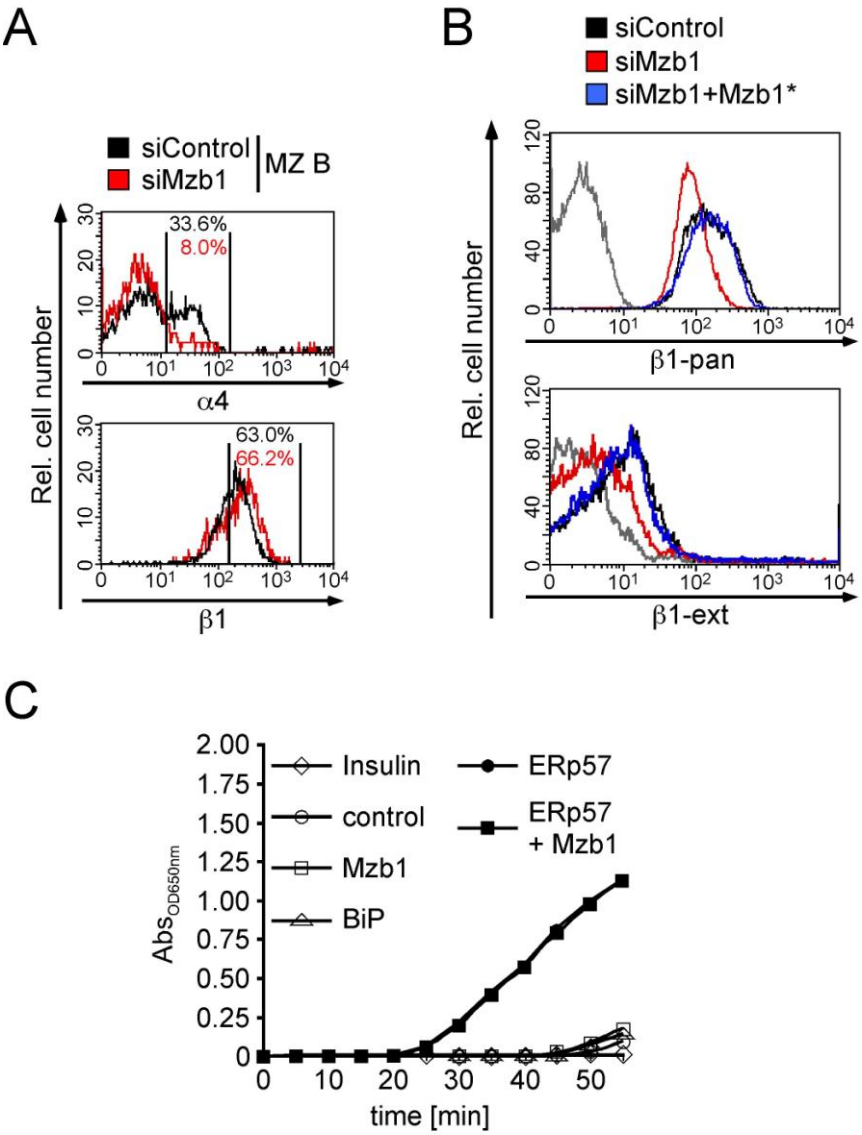

Flach et al., Supplemental Figure S6

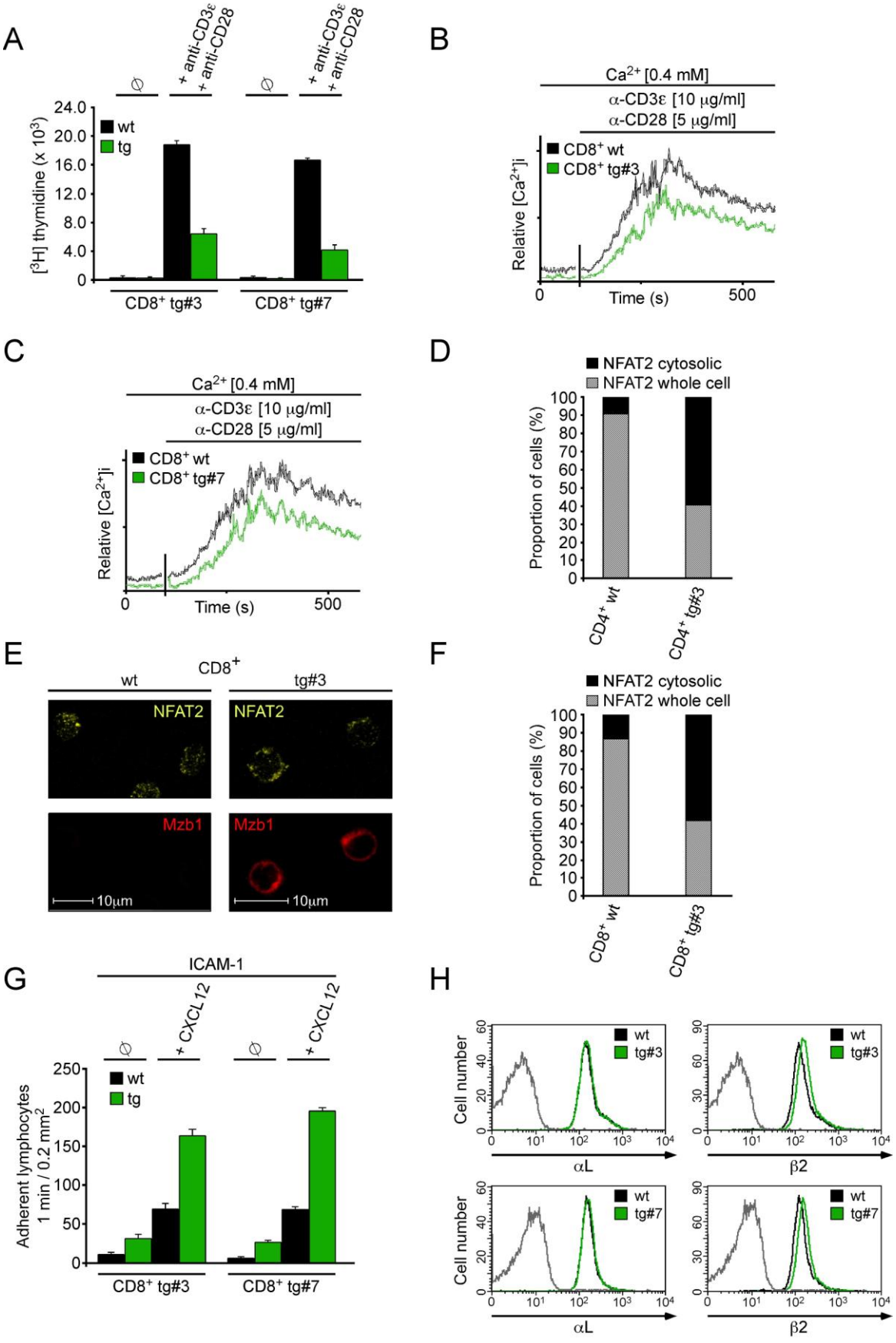

Flach et al., Supplemental Figure S7

Position	Sequence	Mascot Score	MD [ppm]	Modification	Protease
19 - 34	SAGDRVSLSASAPTLD	29	0.21		GluC
19 - 36	SAGDRVSLSASAPTLDDE	70	0.69		GluC
21 - 36	GDRVSLSASAPTLDDE	57	0.46		GluC
22 - 34	DRVSLSASAPTLD	33	0.73		GluC
22 - 36	DRVSLSASAPTLDDE	87	0.06		GluC
23 - 37	RVSLSASAPTLDDEE	64	0.80		GluC
38 - 50	KYSAHMPAHLRCD	21	0.25	MetOx	GluC
38 - 50	KYSAHMPAHLRCD	19	1.90		GluC
51 - 67	ACRAVAFQMGQRLAKAE	21	0.69	MetOx	GluC
68 - 74	AKSHTPD	15	1.55		GluC
68 - 80	AKSHTPDASGLQE	57	0.90	Deamidation	GluC
68 - 80	AKSHTPDASGLQE	49	1.58		GluC
84 - 105	STYTDVLDQTCSQNWQSYGVHE	30	0.58	Deamidation	GluC
84 - 105	STYTDVLDQTCSQNWQSYGVHE	23	0.76		GluC
149 - 156	FGEDQIYE	49	1.08		GluC
157 - 166	AYRQGQANLE	36	0.92		GluC
167 - 180	ALLCGGTHGPCSQE	71	0.20		GluC
181 - 186	ILAQRE	33	1.59		GluC
181 - 186	ILAQRE	33	0.28	Deamidation	GluC
181 - 187	ILAQREE	21	1.81		GluC
181 - 188	ILAQREEL	38	2.76	Deamidation	GluC
181 - 188	ILAQREEL	37	0.26		GluC
21 - 38	GDRVSLSASAPTLDDEEK	19	1.54		Trypsin
22 - 38	DRVSLSASAPTLDDEEK	74	1.73		Trypsin
22 - 48	DRVSLSASAPTLDDEEKYSAHMPAHLR	43	0.22		Trypsin
24 - 38	VSLSASAPTLDDEEK	58	0.95		Trypsin
24 - 48	VSLSASAPTLDDEEKYSAHMPAHLR	18	0.79	MetOx	Trypsin
24 - 48	VSLSASAPTLDDEEKYSAHMPAHLR	17	0.58		Trypsin
39 - 48	YSAHMPAHLR	32	0.53	MetOx	Trypsin
39 - 48	YSAHMPAHLR	30	0.51		Trypsin
54 - 62	AVAFQMGQR	52	0.10		Trypsin
63 - 69	LAKAEAK	26	0.06		Trypsin
70 - 110	SHTPDASGLQELSESTYTDVLDQTCSQ NWQSYGVHEVNQMK	51	1.22	MetOx	Trypsin
70 - 110	SHTPDASGLQELSESTYTDVLDQTCSQ NWQSYGVHEVNQMK	38	0.93		Trypsin
70 - 111	SHTPDASGLQELSESTYTDVLDQTCSQ NWQSYGVHEVNQMKR	21	0.11	MetOx	Trypsin
111 - 119	RLTGPGLSK	44	1.39		Trypsin
111 - 124	RLTGPGLSKGPEPR	40	1.02		Trypsin
112 - 119	LTGPGLSK	33	0.34		Trypsin
112 - 124	LTGPGLSKGPEPR	56	1.19		Trypsin
125 - 137	ISVMISGGPWPNR	64	1.88	Deamidation	Trypsin
125 - 137	ISVMISGGPWPNR	59	1.94		Trypsin
125 - 140	ISVMISGGPWPNRLSK	24	0.89		Trypsin
125 - 140	ISVMISGGPWPNRLSK	31	1.17	MetOx	Trypsin
141 - 159	TCFHYLGEFGEDQIYEAYR	75	0.88	Deamidation	Trypsin
141 - 159	TCFHYLGEFGEDQIYEAYR	52	1.56		Trypsin
160 - 185	QGQANLEALLCGGTHGPCSQEILAQR	48	0.33		Trypsin
160 - 188	QGQANLEALLCGGTHGPCSQEILAQREEL	45	0.23	Deamidation	Trypsin
160 - 188	QGQANLEALLCGGTHGPCSQEILAQREEL	39	0.06		Trypsin

Flach et al., Supplemental Table S1

	beads	α-EBNA	α-MZB1
Gelband 1			
Protein	not detected	Hyou1	Hyou1
Uniprot		Q9JKR6	Q9JKR6
MW (kDa)		111.2	111.2
EmPAI		0.52	9.4
Unique peptides		24	64
Sequence cover. (%)		27	55
Gelband 2			
Protein	not detected	Grp94	Grp94
Uniprot		P08113	P08113
MW (kDa)		92.5	92.5
EmPAI		0.07	1.46
Unique peptides		3	25
Sequence cover. (%)		3	34
Protein	not detected	BiP	BiP
Uniprot		P20029	P20029
MW (kDa)		72.4	72.4
EmPAI		0.27	2.97
Unique peptides		8	31
Sequence cover. (%)		16	49
Protein	not detected	not detected	Calreticulin
Uniprot			P14211
MW (kDa)			48.0
EmPAI			0.62
Unique peptides			10
Sequence cover. (%)			25
Protein	not detected	not detected	Calnexin
Uniprot			P35564
MW (kDa)			67.3
EmPAI			0.28
Unique peptides			7
Sequence cover. (%)			11
Gelband 3			
Protein	not done	Grp94	Grp94
Uniprot		P08113	P08113
MW (kDa)		92.5	92.5
EmPAI		1.64	**35.72**
Unique peptides		32	82
Sequence cover. (%)		34	65
Protein	not done	not detected	Serca2b
Uniprot			O55143
MW (kDa)			114.9
EmPAI			0.03
Unique peptides			3
Sequence cover. (%)			2
Protein	not done	not detected	Integrin b1
Uniprot			P09055
MW (kDa)			88.2
EmPAI			0.07
Unique peptides			4
Sequence cover. (%)			6
Gelband 4			
Protein	BiP	BiP	BiP
Uniprot	P20029	P20029	P20029
MW (kDa)	72.4	72.4	72.4
EmPAI	2.35	7.83	**318.54**
Unique peptides	29	47	76
Sequence cover. (%)	45	58	75
Gelband 5			
Protein	not done	ERp57	ERp57 (Pdia3)
Uniprot		P27773	P27773
MW (kDa)		56.7	56.7
EmPAI		3.29	**26.69**
Unique peptides		27	53
Sequence cover. (%)		43	74
Gelband 6			
Protein	not detected	Pdia6	Pdia6
IPI mouse		IPI00854971	IPI00854971
MW (kDa)		42.9	42.9
EmPAI		0.4	4.41
Unique peptides		6	18
Sequence cover. (%)		18	43

Flach et al., Supplemental Table S2

LEGENDS TO SUPPLEMENTAL FIGURES AND TABLES

Figure S1: Expression, subcellular localization and processing of Mzb1

(A) Quantitative RT-PCR analysis of *Mzb1* transcripts in $B220^{+}CD21^{int}CD23^{hi}$ follicular B cells and $B220^{+}CD21^{hi}CD23^{-}$ MZ B cells. Relative *Mzb1* expression is normalized to *actin* (n=2). (B) RNA-blot analysis of poly-A^{+} RNA from indicated B and T cell lines. Membranes were hybridized with probes specific for *Mzb1* and *OcaB.* (C) Northern blot analysis of poly-A^{+} RNA from adult mice tissues to detect transcripts of *Mzb1*, *Gapdh* and the constant region of *Igκ*. (D) Comparison of amino acid sequences of Mzb1 in chordates. Conserved residues are shaded red, yellow, green or blue, with red indicating the highest sequence conservation. Blue (trypsin digest) and black (GluC digest) lines represent the peptide coverage of murine Mzb1, as identified by mass-spectrometry. The red line marks a signal peptide-derived fragment identified in recombinant Mzb1. Peptidase cleavage sites in murine Mzb1 are indicated by open triangles. (E) Immunohistochemical analysis of Mzb1-GFP or ΔN-Mzb1-GFP expression in NIH 3T3 cells stably transfected with a *Mzb1-GFP* or a *ΔN-Mzb1-GFP* gene construct. Cells were treated for 6 hrs with DMSO or 1μg/ml nocodazole, fixed with paraformaldehyde and incubated with Mzb1- or BAP31-specific antibodies. (F) Indirect immunofluorescence analysis of FACS-sorted MZ B cells, using an anti-Mzb1 antibody, followed by anti-rat Alexa647® secondary antibody. (G) AnnexinV apoptosis assay on control (siControl) and Mzb1-knockdown (siMzb1) K46 B cells. Cells were either kept untreated (left panels) or incubated with tunicamycin (12.5 μg/ml) for 6hrs and 24hrs (middle and right panels). Cells were stained with Annexin V-PE in a buffer containing 7-amino-actinomycin D (7AAD) and analyzed by flow cytometry. Numbers indicate percentages of cell populations in the four quadrants. Data are representative of three independent experiments. (H) Indirect immunofluorescence analysis of freshly sorted $B220^{+}CD21^{int}CD23^{hi}$ FoB cells using anti-Mzb1 and anti-NFAT2 antibodies. (I) Indirect immunofluorescence analysis of freshly sorted, B220-positive splenic FoB cells which have been depleted for MZ B and antibody-secreting B cells ($AA4.1^{-}CD9^{-}CD43^{-}CD4^{-}CD8^{-}$) using anti-Mzb1 and anti-NFAT2 antibodies. (J) Flow cytometric analysis of GFP expression in FoB cells transduced with a

Mzb1-expressing retrovirus and in MZ B cells transduced with a Mzb1-siRNA-expressing retrovirus. FoB cells were either infected in the absence of LPS (left) or infected for 24 hrs in the absence of LPS followed by 24 hrs of stimulation with 10 μg/ml LPS (middle panel). FACS histograms reflect living B220-positive cells. Data are representative of three independent experiments.

Figure S2: Mzb1 regulates Ca^{2+} fluxes and ER Ca^{2+} store content

(A-E) Analysis of experimentally induced Ca^{2+} fluxes in control (siControl), Mzb1-knockdown (siMzb1 #2, #10 and # 29), Mzb1*-rescue (siMzb1+Mzb1*), and mutant Mzb1*-rescue (siMzb1+Mzb1*^{CXXA}) K46 cells. Indo-1AM-loaded cells were treated (A and C) with anti-κ (5 μg/ml), (D) thapsigargin (1 μM) or (B and E) ionomycin (1.4 μM) and increases in free intracellular Ca^{2+} were measured in real time. In parallel to the indicated stimuli, cells were induced by addition of CXCL13 (0.5 μg/ml) (C - E). Data are representative of five independent experiments. (F) Electrophoretic mobility shift assay (EMSA) to detect binding of NFAT in nuclear extracts of serum-starved control (siControl), Mzb1-knockdown (siMzb1), and Mzb1*-rescue (siMzb1+Mzb1*) K46 cells, left untreated or BCR-stimulated (anti-κ; 5 μg/ml) for 30 min. 4 μg of nuclear extract was incubated with radiolabeled oligonucleotides encompassing an Oct1- (loading control) or NFAT-binding site. The specificity of binding was confirmed by 75 fold molar excess of unlabeled oligonucleotides encompassing the same NFAT-binding site (specific competitor). The figure is a representative of three independent experiments. (G) Analysis of NFAT-dependent transcription by determining the activity of a transiently transfected luciferase reporter containing three NFAT-binding sites. Luciferase activity was measured in unstimulated cells (left) or 6 hrs after stimulation of the cells with anti-κ (right). Obtained luciferase values were normalized to co-transfected β-galactosidase and mean values of duplicate stimulations are shown. Error bars indicate SD of the mean. (H) Indirect immunofluorescence using peritoneal B1 B cells transduced with a control- (siControl; left panels) or Mzb1-siRNA-expressing (siMzb1; right panels) retrovirus. After

transduction, GFP-positive cells were enriched by FACS-sorting and cells were stained using anti-Mzb1 and anti-NFAT2 antibody followed by DAPI.

Figure S3: Mzb1 interacts with ERp57 and Grp94

(A-B) Co-immunoprecipitation analysis of total K46 protein extract to detect association of Mzb1 with ERp57 and Grp94 in the absence (10 mM EDTA) or presence (2.5 mM Ca^{2+}) of calcium. (A) Co-immunoprecipitation analysis with anti-ERp57 antibody. (B) Co-immunoprecipitation analysis with anti-Grp94 antibody.

Figure S4: Mzb1 influences antibody secretion

ELISA assay to detect secretion of IgM in supernatants of MZ B cells transduced with a control- or Mzb1-siRNA-expressing retrovirus or FoB cells transduced with a mock- or Mzb1-expressing retrovirus. Retroviral transductions were performed for 12 hrs in the presence of LPS (1 μg/ml), GFP-positive cells were then sorted and stimulated with LPS (1 μg/ml) for an additional 12 hrs before supernatants were used for the assay. Data represent the mean and SD of triplicate samples and data are representative of three independent experiments.

Figure S5: Mzb1-knockdown does not affect CXCR5 surface expression

(A-B) FACS analysis of surface CXCR5 expression on MZ B cells transduced with control- or Mzb1-siRNA-expressing retrovirus (A), and on control- (black line), Mzb1-knockdown (red line) and Mzb1*-rescue (blue line) K46 cells (B). Numbers indicate percentages of cell populations in the four quadrants (A). The solid grey line represents the isotype control (B). Data are representative of three independent experiments (A-B).

Figure S6: Mzb1 regulates integrin-surface expression and integrin-folding in a substrate-specific manner

(A) Flow cytometric analysis of surface integrin levels on MZ B cells transduced with a control- (black line) or Mzb1-siRNA-expressing retrovirus (red line). FACS profiles reflect

living GFP-positive cells and data are representative of three independent experiments. (B) Flow cytometric analysis of surface integrin levels of either pan β1 integrin (upper panel) or the extended, activated form of β1 integrin (lower panel) on control (siControl; black line), Mzb1-knockdown (siMzb1; red line) and Mzb1*-rescue (siMzb1+Mzb1*; blue line) K46 cells. The solid grey line represents the isotype control. (C) Enzymatic activity of GST-ERp57 (positive control), GST-BiP, Mzb1, and GST-ERp57 combined with Mzb1 was measured using the insulin turbidity assay. GST-BiP alone and an input sample lacking enzyme (control) are used as negative controls. As a further control, insulin in the absence of DTT (insulin) was measured in parallel. $Abs_{OD650nm}$ values were collected and plotted as a function of time. Graphs represent three independent experiments.

Figure S7: Ectopic expression of Mzb1 in T cells alters cell proliferation, Ca^{2+} mobilization and integrin-mediated cell-adhesion

(A) Analysis of cell proliferation of CD8-positive splenocytes isolated from wild type (wt) or *Lck-Mzb1* transgenic mice (lines #3 and #7). [^{3}H] thymidine incorporation was determined in cells without (ø) or with stimulation by anti-CD3ε (1 μg/ml) and anti-CD28 (1 μg/ml) for 16 hrs. Data are expressed as the mean [^{3}H] thymidine incorporation of triplicate cultures and are representative of three independent experiments. Error bars indicate SD of the mean. (B-C) Analysis of experimentally induced Ca^{2+} fluxes of CD8-positive splenocytes isolated from control (wt) or *Lck-Mzb1* transgenic mice (line #3 shown in B and line #7 shown in C). Indo-1AM-loaded cells were treated with anti-CD3ε (10 μg/ml) and anti-CD28 (5 μg/ml) and increases in free intracellular Ca^{2+} were measured in real time. Data are representative of four independent experiments with similar results. (D) Quantification of the proportion of wt or Mzb1-transgenic CD4-positive splenic T cells ($n \geq 115$ per genotype) showing NFAT2 protein distributed over the whole cell (hatched bar) or mainly concentrated in the cytosolic compartment (solid bar). (E) Indirect immunofluorescence analysis of FACS-sorted and anti-CD3ε (10 μg/ml) and anti-CD28 (5 μg/ml) -stimulated $CD8^+$ wild type or Mzb1-transgenic T cells (line #3), using an anti-Mzb1 or anti-NFAT2 antibody. (F) Quantification of the

proportion of wt or Mzb1-transgenic CD8-positive splenic T cells ($n \geq 118$ cells per genotype) showing NFAT2 protein distributed over the whole cell (hatched bar) or mainly concentrated in the cytosolic compartment (solid bar). (G) Static adhesion to ICAM-1. Wild type or Mzb1-transgenic $CD8^+$ T cells (lines #3 and #7) were treated with buffer (ø) or stimulated with CXCL12. Assays were performed in triplicate, and data are representative of three independent experiments. Error bars indicate SD of the mean. (H) Flow cytometric analysis of αL and β2 surface integrin levels on control (wt) or Mzb1-transgenic T cells (transgenic line #3 upper panel; transgenic line #7 lower). The solid grey line represents the isotype control. FACS profiles indicate CD8-positive cells, and data are representative of three independent experiments.

Table S1: Processing and subcellular localization of Mzb1

Mass spectrometric analysis of peptides derived from endogenous Mzb1. Endogenous Mzb1 protein was immunoprecipitated with an anti-Mzb1 monoclonal antibody, separated by SDS-PAGE and subjected to in-gel digestion with either trypsin or GluC (V8 protease). The positions of the peptides in the amino acid sequence of the non-processed full-length protein are indicated. The data are consistent with a cleavage of Mzb1 by signal peptidase at positions 19 and 21. However, we cannot rule out a putative additional signal peptidase cleavage site at position 22 since glycine was recently shown to represent a suboptimal cleavage site for GluC (Schilling and Overall, 2008). The mass deviation (MD) to the theoretical peptide mass (note the excellent low to sub ppm MD) and modifications of the peptides (MetOx: oxidation of methionine; Deamidation of glutamine or asparagine) are shown.

Table S2: Proteins detected by LC-MS that co-purify with Mzb1

K46 cells were subjected to formaldehyde cross-linking before cell lysis in order to stabilize dynamic protein-protein interactions. Silver-stained protein bands (Fig. 3 B) specifically enriched by α-Mzb1 IP (compared to isotype-control IP=α-EBNA1 and sepharose beads)

were analyzed by LC-MS. Since Mzb1 binds weakly to IgG heavy chains, we determined the enrichment of co-purifying polypeptides by comparing their amounts in α-Mzb1 versus α-EBNA1 (isotype) IPs using the exponential protein abundance (emPAI) index that can be derived from LC-MS datasets (see supplemental experimental procedures). The emPAI value is directly proportional to the protein content of a given protein in a sample (protein mixture). The data demonstrate that the proteins Hyou1, Grp94, BiP, calreticulin, calnexin, Serca2b, Integrinb1, ERp57 and Pdia6-like can be selectively captured in MZB1-containing protein complexes because they are significantly enriched in the α-MZB1 IP, which for example contains 18-times more Hyou1 protein than the control (gelband 1).

SUPPLEMENTAL EXPERIMENTAL PROCEDURES

Cell culture.

K46 siControl, siMzb1, siMzb1+Mzb1* and siMzb1+Mzb1*^{CXXA} cells were cultured in RPMI 1640 medium (PAA) supplemented with 10% (v/v) heat-inactivated FCS, 1% (v/v) PSG (Gibco) and 56 µM ß-mercaptoethanol (Sigma) at 37°C in a 5% CO_2-gassed atmosphere. To select for stable integration of the Mzb1-siRNA-, the *Mzb1** or the *Mzb1**^{CXXA}-expression plasmids, cells were passaged in selection media containing 1mg/ml active G418 and 1 µg/ml puromycin. Primary MZ B, FoB and B1 cells were maintained in RPMI 1640 media supplemented with 10% (v/v) heat-inactivated FCS, 1% (v/v) PSG (Gibco), 1% (v/v) non-essential-amino-acids (Gibco), 1% sodium pyruvate (Gibco), 10 mM HEPES (Gibco) and 56 µM ß-mercaptoethanol (Sigma) at 37°C in a 5% CO_2-gassed atmosphere.

Mzb1-specific monoclonal antibodies

Affinity-purified, recombinant GST-Mzb1 was used to generate Mzb1-specific monoclonal antibodies. Dr. Elisabeth Kremmer (GSF, Munich) immunized rats with GST-Mzb1, and generated hybridomas which were tested to recognize endogenous as well as recombinant Mzb1 in standard immunoblot and immunofluorescence analyses. From 28 hybridomas, 14 were identified that secrete antibodies with intermediate efficiency of Mzb1 recognition, and 4 hybridomas were found to produce antibody with very high efficiency and specificity of Mzb1 recognition. Monoclonal anti-Mzb1 antibody 2F9 was used for most immunoblot and immunofluorescence assays presented.

Generation of *Lck-Mzb1* transgenic mice

The *Lck-Mzb1* transgenic construct was generated by inserting PCR-amplified mouse *Mzb1* genomic DNA between positions -14 upstream of the translation initiation codon and +141 downstream of the translation stop codon into the *BamHI* site of the vector pLck-hGH (Garvin et al., 1990). Prior to microinjection, plasmid DNA was linearized using a *NotI* restriction site, followed by agarose gel extraction of the linearized fragment. Microinjection was performed

into FVB-derived zygotes and transgenic founders were identified by Southern blot analysis of the tail genomic DNA according to standard protocols. Three independent transgenic lines (tg#3, tg#7 and tg#38) were generated and backcrossed with C57BL/6J wt-mice. Transgenic offspring were determined by PCR of the tail genomic DNA using the transgene-specific primers Lck-forward (5'-AGGGAGCCGAAGTAGACACAG-3') and Lck-reverse (5'-CAGTAGCAACAGTGGCAGAGG-3'). For the experiments, transgenic offspring and their wt littermates of two independent lines (tg#3 and tg#7) were analyzed.

Ca^{2+} mobilization

K46 Mzb1-siRNA cells and the corresponding controls, sorted and retrovirally infected primary FoB (mock, +Mzb1) cells (2 x 10^6/sample) or primary splenic T cells (2 x 10^6/sample) derived from Lck::Mzb1 transgenic mice or wt littermate controls were loaded with 5 μg/ml of Indo-1 AM (Molecular Probes) and 0.5 μg/ml Pluronic® F-127 (Molecular Probes) in RPMI 1640 medium (PAA) containing the indicated Ca^{2+} concentration and supplemented with 1% FCS at 37°C. After 45 min incubation, the cell pellets were resuspended in RPMI 1640 medium plus 1% FCS and kept on ice. Ca^{2+}-flux was induced by addition of goat anti-kappa antibody (5 μg/ml) (Southern Biotechnology), hamster anti-CD3ε antibody (10μg/ml) (clone 145-2C11; nano Tools) combined with hamster anti-CD28 antibody (5μg/ml) (clone 37.51; eBioscience), the SERCA pump inhibitor thapsigargin (Lytton et al., 1991) (1 μM) combined with Ca^{2+} (5 mM), or ionomycin (1.4 μM). If Ca^{2+} was indicated 0 mM, EGTA was added at a final concentration of 3 mM. If stated, cells were co-stimulated with CXCL13 (0.5 μg/ml; R&D Systems). Increases in free intracellular calcium in gated (GFP-positive or CD4-positive or CD8-positive) cell populations were measured in real time on a LSRII flow cytometer (BD Biosciences).

Single cell Ca^{2+} measurement

Ratiometric $[Ca2^{+}]_i$ imaging experiments were performed on K46 Mzb1-siRNA cells and the corresponding control cells or on NIH3T3 cells stably transfected with a mock- or Mzb1-

expression plasmid with Fura-2 as previously described (Zhang et al., 2005). Data were analysed with the Metafluor software (Universal Imaging) and OriginPro 7.5 software (OriginLab) and are expressed as mean values ± s.e.m.

AnnexinV apoptosis assay

AnnexinV apoptosis assay was performed on control and Mzb1-siRNA K46 cells. Cells were either kept untreated or apoptosis was induced by incubation with tunicamycin (12.5 μg/ml; Sigma) for 6hrs or 24hrs, respectively. Annexin V staining was performed according to the manufacturer`s instructions (BD Biosciences) and the samples were analyzed by flow cytometry.

***In vivo* formaldehyde crosslink and immunoprecipitation**

K46 cells were stimulated with thapsigargin (1 μM) and EGTA (3 mM) for 30 min and subjected to an *in vivo* formaldehyde crosslinking reaction as previously described (Guerrero et al., 2006). Briefly, 1% formaldehyde was directly added to the K46 cell culture for 10 min at 37 °C. The crosslinking reaction was quenched for 10 min at 37 °C by addition of 2.5 M glycine at a final concentration of 0.125 M. After cross-linking, cells were collected, washed with ice-cold PBS and frozen at 80 °C prior to lysis. Frozen cells were lysed by sonification in lysis buffer (20mM Tris/Cl, pH 7.4; 10mM EDTA; 1%(w/v) SDS; 5mM Na_3VO_4; 1mM PMSF; 10% v/v protease inhibitor cocktail (Sigma)), and cellular debris was removed by centrifugation. Clarified lysate was diluted 1:5 with ice cold IP buffer (20mM Tris/Cl, pH 7.4; 10mM EDTA; 5mM Na_3VO_4; 0.2% NP-40; 0.5% sodium deoxycholate (DOC); 1mM PMSF; protease inhibitors) and an immunoprecipitation was performed using Protein A/G-purified anti-Mzb1 antibodies directly coupled to CNBr-activated Sepharose-beads (GE Healthcare). As controls, 4B-Sepharose beads and anti-EBNA Sepharose-beads were used. After binding, the beads were washed 5 times with 20 bed volumes of IP buffer and the proteins were eluted in sample buffer. The binding reaction was allowed to proceed for 5 h at 4°C.

Liquid chromatography mass spectrometry

Proteins were separated on 4-12 % Bis-Tris SDS gels (NuPAGE, Invitrogen) and stained with silver. Individual bands were excised and subjected to in-gel digestion using either trypsin (Promega) or GluC (*S. aureus* protease V8, Roche), essentially as described (Shevchenko et al., 2006). For the analysis of Mzb1 GluC digestion conditions (12.5 ng/µl in 20 mM Hepes-KOH, pH 7.9; 25°C, over night) were adjusted for preferential cleavage carboxyterminal to glutamate, but enabling some residual cleavage carboxyterminal to aspartate (Schilling and Overall, 2008). Prior to LC-MS analysis peptide mixtures were desalted using STAGE tips as previously described (Rappsilber et al., 2003; Rappsilber et al., 2007). All experiments were analyzed by nanoscale-LC (MDLC, GE Biosciences) coupled to a 7-Tesla linear ion-trap Fourier-transform ion cyclotron resonance mass spectrometer (LTQ-FT Ultra, Thermo Electron, Germany) equipped with a nanoelectrospray source (Proxeon, Denmark). The 15 cm fused silica emitter with an inner diameter of 75 µm and a tip diameter of 8 µm (New Objective, USA) was packed in-house with reverse-phase ReproSil-Pur C18-AQ 3 µm resin (Dr. Maisch GmbH, Germany). Peptides were eluted from an analytical column by a linear gradient running from 2 to 42% (v/v) acetonitrile (in 0.5% acetic acid) with a flow rate of 250 nl/min in 35 minutes and sprayed directly into the orifice of the mass spectrometer. We used the following parameters for information dependent acquisition of MS and MS/MS spectra. Survey full-scan MS spectra (m/z 350 – 1800) were acquired in the Fourier transform ion cyclotron resonance Ultra (FT-ICR Ultra) cell with resolution R = 100,000 at m/z = 400 with a target value of 1,000,000 ions allowing a maximum fill-time of 1200 ms. The five most intense ions were sequentially isolated and fragmented in the linear ion trap by CID (collision induced dissociation) at a target value of 10,000 (maximum fill-time = 250 ms). Target ions selected for MS/MS were dynamically excluded for 90 s. Total cycle time was 2.0 to 2.5 s. The general mass spectrometric conditions were: spray voltage, 2.3 kV; no sheath and auxiliary gas flow; ion transfer tube temperature, 120°C; helium collision gas pressure, 1.3 mTorr; normalized collision energy

using wide-band activation mode; 30% for MS^2. Ion selection thresholds were 500 counts for MS/MS with an activation q = 0.25 and activation time of 30 ms.

Mass Spectrometry Data analysis

FT-MS data were processed into peak lists using the open source software DTA SuperCharge (http://msquant.sourceforge.net/) and searched with Mascot 2.2 (Matrix Science, UK) against the mouse International Protein Index protein database (IPI, http://www.ebi.ac.uk/IPI/IPIhelp.html) supplemented with frequently observed contaminants and concatenated with reversed copies of all sequences as described (Mittler et al., 2009). For tryptic digestions enzyme specificity was set to trypsin, allowing for cleavage N-terminal to proline and between aspartic acid and proline. For GluC digests we allowed cleavage C-terminal to glutamate and aspartate (Schilling and Overall, 2008). Carbamidomethyl cysteine was set as fixed and oxidized methionine, N-acetylation, deamidation of asparagine and glutamine as well as loss of ammonia from N-terminal glutamine as variable modifications. For experiments employing formaldehyde-assisted Mzb1 protein complex purification formylation of serine, threonine and lysine was used as an additional variable modification. The ion score cut-off was set to 15 and maximum allowed mass deviation MMD (Zubarev and Mann, 2007) for monoisotopic precursor ions and MS/MS peaks was restricted to 10 ppm and 0.5 Da, respectively. Protein identifications were further analyzed and manually verified by the use of MSQuant (http://msquant.sourceforge.net/). The minimum required peptide length was set to 6 amino acids and the MMD to 5 ppm. Proteins were only considered to be identified with a Mascot score of 50 and at least two different (at sequence level) peptides, thereof one can be uniquely assigned to the respective protein sequence.

In order to approximate the abundance of a protein in a given sample or gel slice we used the emPAI (exponential protein abundance index) (Ishihama et al., 2005; Ishihama et al., 2008) function implemented into Mascot 2.2 (http://www.matrixscience.com/help/quant_empai_help.html). The emPAI index formula is: emPAI= $10^{(N_{observed}/N_{observable})} -1$, where $N_{observed}$ is the number of experimentally observed

peptides and $N_{observable}$ the number of calculated observable peptides of a protein. The latter is a function of the protein molecular weight and amino acid composition, which determines the number of tryptic peptides that can be detected by a given LC-MS setup. This normalization is important since larger proteins lead to more peptides and not all peptides bind or separate well on C18 reversed phase columns or fall into the detection range of the mass spectrometer (e.g. m/z=300 to 1800). The emPAI value is directly proportional to the protein content of a given protein in a sample (protein mixture). A ten-fold difference in the emPAI value corresponds to a tenfold difference in the protein concentration for a given protein in the sample.

Microsomal preparations, Proteinase K digest and size exclusion chromatography

K46 cytosolic (S100) and microsomal (Micro) fractions were prepared as previously described (Oh and Turner, 2006). Aliquots of this preparation (~50 µg of protein) were incubated in the presence or absence of 1% Triton X-100 for 10 min on ice followed by treatment of 2 mg/mL proteinase K on ice for 30 min. The reaction was stopped by addition of PMSF (30 mM final) as well as protein precipitation by trichloroacetic acid (TCA) and subsequently, samples were attributed to SDS-PAGE and immunoblotting. For size exclusion chromatography, microsomal fractions were prepared in the presence of 2.5 mM Ca^{2+} (w/o EDTA) or its absence (10 mM EDTA) as described (Huber et al., 2000). The samples were separated on an analytical HR10/30 Superdex 200 (Amersham/GE Healthcare) column followed by an immunoblot analysis using Mzb1-specific antibody.

Enzyme-linked immunosorbent assay (ELISA) and ELISpot assay.

Antibodies used for ELISA and ELISpot assays were goat anti-mouse IgM to coat the plates and biotinylated goat anti-IgM as a secondary detection step (Southern Biotechnology Associates). Purified mouse monoclonal IgM (Southern Biotechnology Associates) was used as a standard for the quantification of immunoglobulin concentrations. To develop the ELISAs, streptavidin–alkaline phosphatase conjugate (Southern Biotechnology Associates)

was used, followed by 4-Nitrophenyl phosphate disodium salt hexahydrate (Sigma) substrate reaction. ELISpot assays were done on MultiScreen-HA filter plates (Millipore). Typically, 2 x 10^4 to 3 x 10^2 (2-fold dilutions) sorted, retrovirally infected (GFP-positive) cells were incubated in 0.2 ml cell culture medium supplemented with LPS (1 μg/ml) on precoated plates for 4 h at 37°C. Development of spots with alkaline phosphatase was performed as described (Sedgwick and Holt, 1986).

Sybr green-based real-time PCR.

Mzb1, *Ccl22*, *Bcl2a1a* (*A1)* and *Bcl2l1* (*Bcl-xL)* mRNA expression levels were measured using Sybr green-based qRT PCR as previously described (Sustmann et al., 2008). Primers were used at 100 nM, and the sequences were as follows: Mzb1-forward 5´-TGC CAC TGT TGC TAC TGT TCG GGT-3´; Mzb1-reverse 5´-GAG TGT GAG ATT TAG CCT CTG CTT TCG-3´; Bcl-xL-forward 5´-GTG CGT GGA AAG CGT AGA CAA-3´; Bcl-xL-reverse 5´-GTT CCC GTA GAG ATC CAC AAA AGT-3´; Ccl22-forward 5´-CTA CCC TGC GTG TCC CAC TCC TG-3´; Ccl22-reverse 5´-GAT GGC AGA GGG TGA CGG ATG TAG TC-3´; A1-forward 5´-AAG AGC AGA TTG CCC TGG ATG TAT GT-3´; A1-reverse 5´-CAG AAA AGT CAG CCA GCC AGA TTT G-3´.

Immunohistochemistry

FACS-sorted and retrovirally infected (GFP-positive) FoB, MZ B and B1 B cells, as well as stimulated $CD4^+$ or $CD8^+$ Mzb1-transgenic or wild type T cells were subjected to standard indirect immunofluorescence (Hewitt et al., 2009), utilizing Mzb1 and NFAT2 specific (ImmunoGlobe, Himmelstadt) antibodies, followed by chicken antibody to rat IgG conjugated to Alexa Fluor 647 (Invitrogen) or goat antibody to rabbit IgG conjugated to Alexa Fluor 568 (Invitrogen), respectively. NIH 3T3 fibroblasts stably expressing Mzb1-GFP or ΔN-Mzb1-GFP were either treated with 1 μg/mL nocodazole or DMSO at 37° C, 5% CO_2 for 6 hrs (Lee et al., 1989) and subjected to indirect immunofluorescence utilizing Mzb1 and Bap31 specific antibodies followed by chicken antibody to rat IgG conjugated to Alexa Fluor 647 (Invitrogen) or goat antibody to rabbit IgG conjugated to Alexa Fluor 568 (Invitrogen), respectively.

Slides were analyzed on a Leica SP2 UV Confocal Microscope (Leica Microsystems, Wetzlar, Germany) with the corresponding Leica LCS Version 2.61 Computer software.

Fluorescence lifetime imaging (FLIM)

NIH 3T3 cells and NIH 3T3 cells stably expressing FLAG-Mzb1 were transiently transfected with 0.25 μg of the yellow cameleon YC4.2er (Luik et al., 2008) using an Amaxa® electroporator (Lonza, Walkersville, MD) according to the manufacturer's protocol and plated onto a 35 mm glass petri-dish. 24 hrs after transfection, cells were bathed in an isotonic buffer (155 mM NaCl, 4.5 mM KCl, 1 mM $MgCl_2$, 10 mM D-glucose, 5 mM HEPES, pH 7.35) containing 2 mM $CaCl_2$ and imaged. Fluorescence Lifetime Imaging Microscopy images were taken with a two-photon home built laser scanning microscope equipped with the Becker & Hickl SPC830 card, (Becker & Hickl GmbH, Berlin, Germany). Excitation provided by the Mai Tai two-photon self-modelocked laser (Spectra-Physics, Newport Corporation, Santa Clara, CA) with a repetition rate of 80 MHz was set to 820nm. The average power before the objective used was ~30-40mW. The laser scanning beam is raster scanned using x-y galvano-scanning mirrors (model 6350; Cambridge Technology, Watertown, MA) driven by the ISS 3-axis card (ISS, Champaign-Urbana, IL) for synchronization. A Zeiss C-Apo 40X (1.2 N.A.), water-immersion objective lens was used for the measurement because of its exceptionally long working distance (230 μm). A 470/30nm filter was placed before the photomultiplier (model H7422P-40, Hamamatsu Photonics, Bridgewater, NJ) to select the emission of CFP. A fluorescein sample at pH 9.0 (Molecular Probes Invitrogen, Carlsbad, CA) served to calibrate the instrument and compensate for its response function. Images were taken at 256x256 pixels with scanning areas from 76 × 76 μm to 46 × 46 μm, comprised a total of 60 integrated frames per image and were processed by the SimFCS software (Laboratory of Fluorescence Dynamics, UC Irvine, CA). In order to measure the lifetime of the YC4.2er in its Ca^{2+} free state as well as in its condition of fully bound Ca^{2+}, the $[Ca^{2+}]_{ER}$ of NIH 3T3 cells was calibrated to an external buffer containing either 0 mM Ca^{2+}(2 mM $MgCl_2$, 70 mM K aspartate, 40 mM KCl, 10 mM HEPES, 20 mM EGTA, pH 7.35) or 20

mM Ca^{2+} (20 mM $CaCl_2$, 2 mM $MgCl_2$, 110 mM K aspartate, 10 mM HEPES, pH7.35). Therefore, the plasma membrane of NIH 3T3 cells was permeabilized by addition of 50 μg digitonin and $[Ca^{2+}]_{ER}$ was allowed to equilibrate for 20 min with the help of 10 μM ionomycin. The data obtained was analysed by the phasor approach (Digman et al., 2008), in which data was subjected to phasor transformation and analysed using the Globals for Images software available at www.lfd.uci.edu.. For every single cell, the fraction of pixels belonging to high calcium regions, i.e. regions showing a short lifetime of CFP due to its quenched state, was transformed into a molar $[Ca^{2+}]_{ER}$, taking into account the YC4.2er-specific dissociation constant K_D (819 μM), the Hill coefficient *n* (0.54) (Luik et al., 2008) and the acquired calibration data for YC4.2er in its Ca^{2+} free (0 mM) as well as in its fully bound Ca^{2+} state (20 mM).

GST pull-down assays

Purification of recombinant GST fusion proteins and recombinant Mzb1 was performed as previously described (Li and Camacho, 2004). Binding of recombinant Mzb1 to GST-ERp57 or GST-BiP fusion protein(s) was performed at 4°C for 2 hrs in the presence of glutathione Sepharose 4B (GE Healthcare Bio-Sciences AB) in binding buffer containing in mM 10 Tris-HCL; pH 8.0; 70 KCL; 2 $MgCl_2$; 50 μM EGTA; 5% BSA and protease inhibitors. Proteins bound to glutathione Sepharose beads were washed three times in buffer containing 0.2 M Tris-HCL; pH 8.0; 0.1% Triton X-100; 70 mM KCl; 2 mM $MgCl_2$; 50 mM EGTA and protease inhibitors. Proteins were competitively eluted using elution buffer containing 20 mM glutathione and 100 mM Tris-HCL, pH 8.0 at 22°C for 10 min. Proteins were resolved by 4% - 12% gradient SDS-PAGE and visualized by immunoblot. GST pull-down assays for recombinant human β1 integrin (source: VLA-4; R&D Systems) in the absence (10mM EDTA) or presence (2.5mM Ca^{2+}) of calcium were performed as described above.

Static adhesion assay and LFA-1/VLA-4 affinity modulation assay

The static adhesion assay was performed as previously described (Bolomini-Vittori et al., 2009). Briefly, retrovirally infected and FACS-sorted (GFP-positive) MZ B cells or FACS-sorted $CD4^+$ or $CD8^+$ transgenic or wild type splenic T cells were resuspended at 5 x 10^6/ml in RPMI 1640 containing 0.5 % BSA. Adhesion assays were performed on 18-well-1μ-slides (Ibidi) coated overnight at 4°C with either murine ICAM-1-FC (1 μg/ml in PBS; R&D Systems) or with murine VCAM-1-FC (1 μg/ml in PBS; R&D Systems). Cell suspension (20 μl) was added to the wells and stimulated for 1 min at 37°C with either CXCL12 (1.0 μg/ml; R&D Systems) or CXCL13 (1.0 μg/ml; R&D Systems). Wells were washed carefully three times with RPMI 1640 containing 0.5 % BSA, cells were fixed in 1.5 % glutaraldehyde in PBS and cells were counted. The LFA-1/VLA-4 affinity modulation assay was performed as previously described (Sebzda et al., 2002). Briefly, retrovirally infected MZ B cells were incubated with soluble murine ICAM-1-Fc (100 μg/ml; R&D Systems) or soluble murine VCAM-1-Fc (100 μg/ml; R&D Systems) for 30 min at 37 °C with or without CXCL13 (0.5 μg/ml; R&D Systems). Cells were stained with human Fc-specific PE-conjugated goat anti-human IgG (Jackson Immunoresearch Laboratories) and fluorescence was detected with a FACSCalibur (Becton Dickinson) flow cytometer.

Insulin turbidity assay

The insulin turbidity assay was performed as previously described (Li and Camacho, 2004). In brief, the insulin stock solution (10 mg/ml; Sigma) was diluted to 1 mg/ml with a buffer containing 100 mM KAc, pH 7.5 and 2 mM EDTA. The final reaction volume was adjusted to 1 ml after purified GST-ERp57, GST-BiP, Mzb1, or a combination of GST-ERp57 and Mzb1 were added (0.8 μM final concentration of each protein). The reaction was initiated by adding 3 μl of 100 mM DTT. Abs_{650nm} was measured every 5 min in a BioPhotometer plus (Eppendorf). Enzyme activity was defined by measuring the slope of the linear portion of the absorbance curve (ΔAbs_{650nm} / min).

VLA-4 reduction assay

Reactions were set up in a final volume of 20 μl containing either 1.13 μg of recombinant human VLA-4 (R&D Systems) alone or in combination with 0.4 μM recombinant murine Mzb1 and/or recombinant murine GST-ERp57 in a buffer containing 2 mM EDTA and 100 mM KCl. Reduction of VLA-4 was initiated by addition of 5 μM DTT and the reaction proceeded for 15 min at RT. In order to stop further reduction of VLA-4, the reduction equivalent DTT was diluted in 800 μl of IP buffer (20 mM Tris-HCl; pH 7.4; 10 mM EDTA; pH 8.0; 5 mM Na_3VO_4; 0.2% NP40; 0.5% DOC supplemented with 1mM PMSF and protease inhibitors). Subsequently, reduced β1 integrin was immunoprecipitated by an activation state-specific anti-β1 antibody, clone 9EG7 (Bazzoni et al., 1995) (BD Pharmingen, Franklin Lakes, NJ), and proteins were resolved by 15% SDS-PAGE and visualized by immunoblot using α-human CD29 (BD Pharmingen, Franklin Lakes, NJ).

SUPPLEMENTAL REFERENCES

Bazzoni, G., Shih, D.T., Buck, C.A., and Hemler, M.E. (1995). Monoclonal antibody 9EG7 defines a novel beta 1 integrin epitope induced by soluble ligand and manganese, but inhibited by calcium. J Biol Chem *270*, 25570-25577.

Bolomini-Vittori, M., Montresor, A., Giagulli, C., Staunton, D., Rossi, B., Martinello, M., Constantin, G., and Laudanna, C. (2009). Regulation of conformer-specific activation of the integrin LFA-1 by a chemokine-triggered Rho signaling module. Nat Immunol *10*, 185-194.

Digman, M. A., Caiolfa, V. R., Zamai, M., and Gratton, E. (2008). The phasor approach to fluorescence lifetime imaging analysis. Biophys J *94*, L14-16.

Garvin, A.M., Abraham, K.M., Forbush, K.A., Farr, A.G., Davison, B.L., and Perlmutter, R.M. (1990). Disruption of thymocyte development and lymphomagenesis induced by SV40 T-antigen. Int Immunol *2*, 173-180.

Guerrero, C., Tagwerker, C., Kaiser, P., and Huang, L. (2006). An integrated mass spectrometry-based proteomic approach: quantitative analysis of tandem affinity-purified in vivo cross-linked protein complexes (QTAX) to decipher the 26 S proteasome-interacting network. Mol Cell Proteomics *5*, 366-378.

Hewitt, S. L., Yin, B., Ji, Y., Chaumeil, J., Marszalek, K., Tenthorey, J., Salvagiotto, G., Steinel, N., Ramsey, L. B., Ghysdael, J.*, et al.* (2009). RAG-1 and ATM coordinate monoallelic recombination and nuclear positioning of immunoglobulin loci. Nat Immunol *10*, 655-664.

Huber, M., Hughes, M. R., and Krystal, G. (2000). Thapsigargin-induced degranulation of mast cells is dependent on transient activation of phosphatidylinositol-3 kinase. J Immunol *165*, 124-133.

Ishihama, Y., Oda, Y., Tabata, T., Sato, T., Nagasu, T., Rappsilber, J., and Mann, M. (2005). Exponentially modified protein abundance index (emPAI) for estimation of absolute protein amount in proteomics by the number of sequenced peptides per protein. Mol Cell Proteomics *4*, 1265-1272.

Ishihama, Y., Schmidt, T., Rappsilber, J., Mann, M., Hartl, F. U., Kerner, M. J., and Frishman, D. (2008). Protein abundance profiling of the Escherichia coli cytosol. BMC Genomics *9*, 102.

Lee, C., Ferguson, M., and Chen, L. B. (1989). Construction of the endoplasmic reticulum. J Cell Biol *109*, 2045-2055.

Li, Y., and Camacho, P. (2004). Ca2+-dependent redox modulation of SERCA 2b by ERp57. J Cell Biol *164*, 35-46.

Luik, R. M., Wang, B., Prakriya, M., Wu, M. M., and Lewis, R. S. (2008). Oligomerization of STIM1 couples ER calcium depletion to CRAC channel activation. Nature *454*, 538-542.

Lytton, J., Westlin, M., and Hanley, M. R. (1991). Thapsigargin inhibits the sarcoplasmic or endoplasmic reticulum Ca-ATPase family of calcium pumps. J Biol Chem *266*, 17067-17071.

Mittler, G., Butter, F., and Mann, M. (2009). A SILAC-based DNA protein interaction screen that identifies candidate binding proteins to functional DNA elements. Genome Res *19*, 284-293.

Oh, Y. S., and Turner, R. J. (2006). Protease digestion indicates that endogenous presenilin 1 is present in at least two physical forms. Biochem Biophys Res Commun *346*, 330-334.

Rappsilber, J., Ishihama, Y., and Mann, M. (2003). Stop and go extraction tips for matrix-assisted laser desorption/ionization, nanoelectrospray, and LC/MS sample pretreatment in proteomics. Anal Chem *75*, 663-670.

Rappsilber, J., Mann, M., and Ishihama, Y. (2007). Protocol for micro-purification, enrichment, pre-fractionation and storage of peptides for proteomics using StageTips. Nat Protoc *2*, 1896-1906.

Schilling, O., and Overall, C. M. (2008). Proteome-derived, database-searchable peptide libraries for identifying protease cleavage sites. Nat Biotechnol *26*, 685-694.

Sebzda, E., Bracke, M., Tugal, T., Hogg, N., and Cantrell, D. A. (2002). Rap1A positively regulates T cells via integrin activation rather than inhibiting lymphocyte signaling. Nat Immunol *3*, 251-258.

Sedgwick, J.D., and Holt, P.G. (1986). The ELISA-plaque assay for the detection and enumeration of antibody-secreting cells. An overview. J Immunol Methods *87*, 37-44.

Shevchenko, A., Tomas, H., Havlis, J., Olsen, J. V., and Mann, M. (2006). In-gel digestion for mass spectrometric characterization of proteins and proteomes. Nat Protoc *1*, 2856-2860.

Sustmann, C., Flach, H., Ebert, H., Eastman, Q., and Grosschedl, R. (2008). Cell-type-specific function of BCL9 involves a transcriptional activation domain that synergizes with beta-catenin. Mol Cell Biol *28*, 3526-3537.

Zhang, S.L., Yu, Y., Roos, J., Kozak, J.A., Deerinck, T.J., Ellisman, M.H., Stauderman, K.A., and Cahalan, M.D. (2005). STIM1 is a Ca2+ sensor that activates CRAC channels and migrates from the Ca2+ store to the plasma membrane. Nature *437*, 902-905.

Zubarev, R., and Mann, M. (2007). On the proper use of mass accuracy in proteomics. Mol Cell Proteomics *6*, 377-381.